Integrating Subsystem Architecture Sizing and Analysis into the Conceptual Aircraft Design Phase

Cooperation between GA Tech's Aerospace Systems Design Laboratory (ASDL) and PACE

Imon Chakraborty
Senior Graduate Researcher, ASDL

David Trawick
Graduate Researcher, ASDL

Dimitri Mavris
Boeing Regents Professor of Advanced Aerospace Systems Analysis & Director, ASDL

Mathias Emeneth
Senior Business Development Manager, PACE America

Alexander Schneegans
Managing Partner & Co-Founder, PACE GmbH, President, PACE America

PACEDAYS 2014 – Berlin, Germany

References & Timeline

The current presentation is based on:

- Chakraborty, I., Trawick, D., Mavris, D.N., Emeneth, M., and Schneegans, A., "A Requirements-driven Methodology for Integrating Subsystem Architecture Sizing and Analysis into the Conceptual Aircraft Design Phase," AIAA Aviation 2014 Conference, Atlanta, GA, June 16-20, 2014, AIAA-2014-3012

- Chakraborty, I., Mavris, D.N., Emeneth, M., and Schneegans, A., "An Integrated Approach to Vehicle, Propulsion System, and Subsystem Sizing - Application to the All Electric Aircraft" Proceedings of the Institution of Mechanical Engineers, Part G: Journal of Aerospace Engineering, **(in review)**

The previous work with Pace (PACEDays 2013) was documented in

- Chakraborty, I., Mavris, D.N., Emeneth, M., and Schneegans, A., "A Methodology for Vehicle and Mission Level Comparison of More Electric Aircraft Subsystem Solutions - Application to the Flight Control Actuation System," Proceedings of the Institution of Mechanical Engineers, Part G: Journal of Aerospace Engineering, DOI: 10.1177/0954410014544303

- Chakraborty, I., Mavris, D.N., Emeneth, M., and Schneegans, A., "A System and Mission Level Analysis of Electrically Actuated Flight Control Surfaces using Pacelab SysArc," AIAA Science and Technology Forum and Exposition (SciTech) 2014, National Harbor, Maryland, Jan 13-17, 2014, AIAA-2014-0381

Agenda

- Introduction and Motivation
- Subsystems
- Implementation and Architecture Application
- Summary

Aircraft Subsystems – Conventional and All Electric

- Aircraft and equipment systems and subsystems are essential for the performance, safety, controllability and comfort

Conventional Subsystems Architecture (CSA)

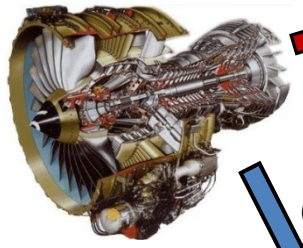

Propulsive power

Non-propulsive (secondary) power "off-takes"

- Bleed air (pneumatic)
  - ECS
  - IPS
- Shaft-power (mechanical)
  - GB
    - P → Hydraulic power
      - Flight controls
      - Landing gear
      - Thrust reversers
      - Wheel braking
      - Ground steering
    - G → Electric power
      - Avionics
      - Lighting
      - Galleys & IFE

- "Bleedless" architecture
- Hydraulics removed
- "Power on Demand"

Electric Subsystems Architecture (ESA)

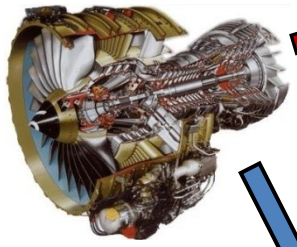

Propulsive power

Non-propulsive (secondary) power "off-takes"

- Shaft-power (mechanical)
  - GB
    - G → Electric power
      - ECS
      - IPS
      - Avionics
      - Lighting
      - Galleys & IFE
      - Flight controls
      - Landing gear
      - Thrust reversers
      - Wheel braking
      - Ground steering

GB: Gearbox
P: Pump
G: Generator

IFE: In-Flight Entertainment
IPS: Ice Protection Systems
ECS: Environmental Control System

Image: www.cfmaeroengines.com

More Electric Aircraft (MEA) – An Intermediate Step

- Due to technological risk, the transition to All Electric Aircraft (AEA) will be progressive
  - *More* Electric Aircraft (MEA) will appear in between
  - *Some* subsystems, but not *all*, will be electric
- Such aircraft have already entered service – Airbus A380 and Boeing 787
- Question: Why do the A380 and B787 have different *electrified* subsystems?
- Question: How should the MEA designer decide which subsystems to *electrify*?

Two in-service More Electric Aircraft

Airbus A380

- **Electrohydrostatic Actuators (EHA)**
- **Electrical Backup Hydraulic Actuators (EBHA)**
- **Electric thrust reverser actuation system (ETRAS)**

Boeing 787

- **Electric (bleedless) ECS architecture**
- **Electric wing ice protection system (WIPS)**
- **Electro Mechanical Brake System (EMBS)**

Consideration of Subsystems in Aircraft Conceptual Design

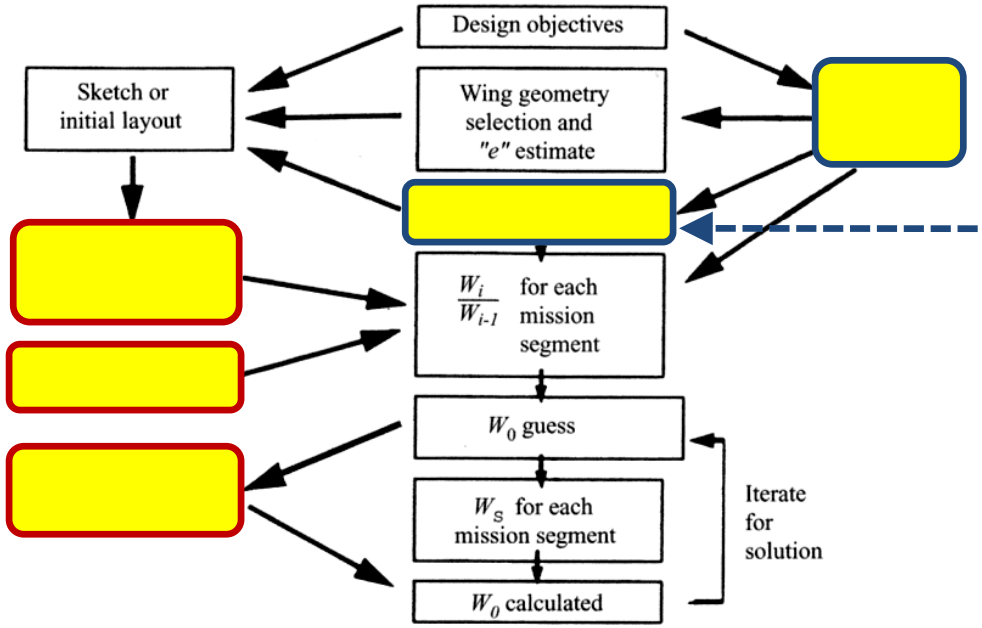

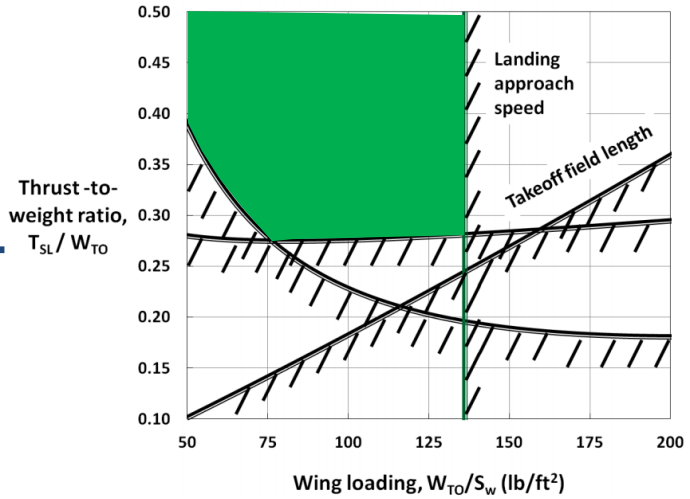

(Notional curves are shown. B737 and A320 points were plotted based on public domain information)

Refined sizing method (Raymer, Aircraft Design: A Conceptual Approach, 4th ed.[1])

- Conceptual phase commercial aircraft sizing is driven by the design requirements:
  - Payload & range requirements
  - Operational requirements (TOFL, Vapp, CRMACH, etc.)
- The aircraft subsystems affect this process
  - Aircraft empty weight (OEW)
  - Engine SFC (shaft-power and bleed extraction)
  - Drag increments (ram air inlets, etc.)

Integrating Subsystems Design in the Conceptual Design Phase

- For conventional subsystems, the conceptual phase designer has access to a vast historical database of information
- This database and regression equations provide a starting point for estimation of subsystem weights

Weight of flight control system (GD method)[2]

$$W_{fc} = 56.01\ \{(W_{TO})(\bar{q}_D)/100{,}000\}^{0.576}$$

Weight of hydraulic, pneumatic, and electrical systems (Torenbeek method)[2]

$$W_{hps} + W_{els} = 0.0078(W_E)^{1.2},$$

where: W_E is the empty weight in lbs

- The conceptual phase designer of AEA / MEA
  - Will not have access to such a historical database or regression equations
  - Will have to account for significant interactions among subsystems
- Conceptual phase design of AEA/MEA can be facilitated through a methodology where
  - subsystem sizing/analysis is done in parallel with that of vehicle and propulsor
  - subsystem characteristics are fed back into vehicle and propulsor analyses

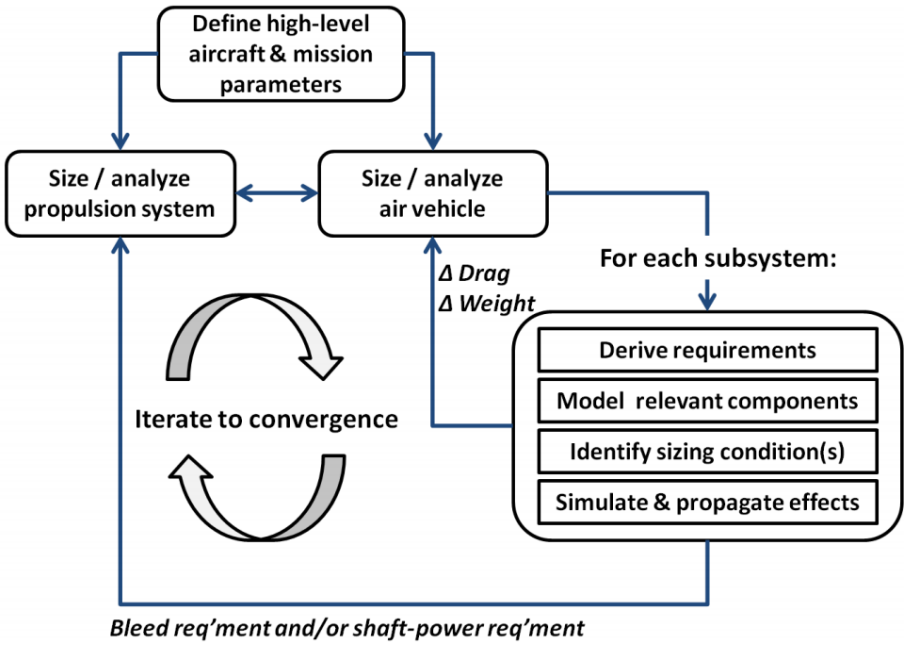

Objectives and Proposed Approach

1. Develop / identify methods suitable for subsystem sizing in conceptual design phase

2. Integrate methods into a framework that allows comparison of the vehicle and mission level effects of CSA and ESA architectures

3. Demonstrate and evaluate the effect of "cycling" the design to capture the "snowball" effects of subsystem architecture changes

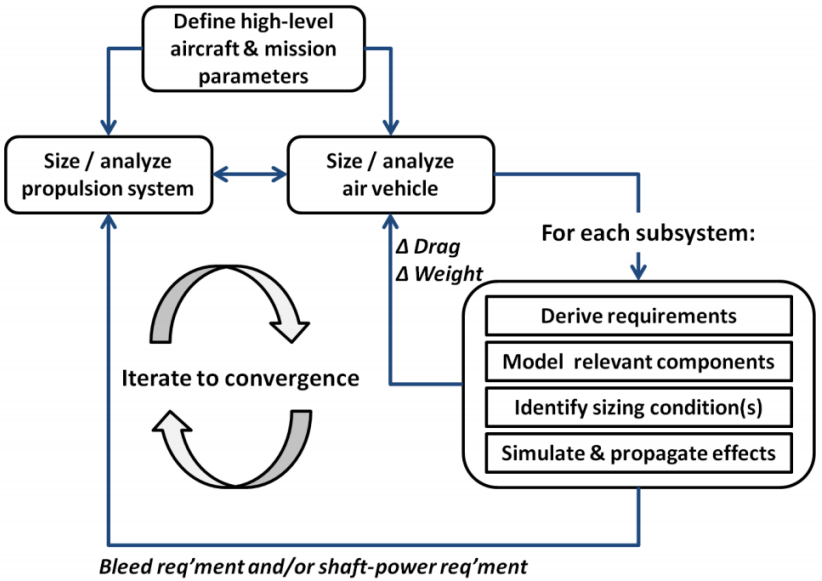

Test case: single-aisle narrow-body aircraft

Parameter	Symbol	Value	
Wing reference area	S_w	124.8 m^2	(1,343 ft^2)
" span	b_w	34.3 m	(112.6 ft)
" sweep (25 % chord)	$\Lambda_{c/4}$	25.02 °	
" aspect ratio	A_w	9.2	
" taper ratio	λ_w	0.21	
" loading	W_{TO}/S_w	622.5 kg/m^2	(127.5 lb/ft^2)
Sea-level static thrust	T_{SL}	242.9 kN	(54,600 lbf)
Thrust-to-weight ratio	T_{SL}/W_{TO}	0.3189	
Operating Empty Weight	OEW	41,871 kg	(92,310 lb)
Maximum Takeoff Weight	MTOW	77,478 kg	(171,201 lb)
Payload	W_{PL}	14,987 kg	(33,040 lb)

Subsystem/function	CSA	ESA
Actuation subsystems		
Control surface actuation	Hydraulic	Electrohydrostatic + Electromechanical
Landing gear actuation, braking, nose-wheel steering	Hydraulic	Electromechanical
Environmental control system	Pneumatic	Electric
Ice protection system		
Wing ice protection	Pneumatic	Electrothermal
Nacelle ice protection	Pneumatic	Electrothermal
Taxiing	Engine thrust	Electric

Agenda

- Introduction and Motivation
- Subsystems
- Implementation and Architecture Application
- Summary

Control Surface Actuation – Actuation Loads

Flight Conditions

- Ailerons: FAR 25.349 – Rolling conditions (V_A, V_C, V_D)
- Elevators: FAR 25.255 – Out-of-trim characteristics
- Rudder: FAR 25.149 – Minimum control speed (V_{MCA})
  FAR 25.351 – Yaw maneuver conditions
- Flight spoilers: Emergency descent at design dive speed (V_D)
- Ground spoilers: Extension at max rated tire speed
- High-lift devices: Extension at max flap extension airspeed (V_{FE})

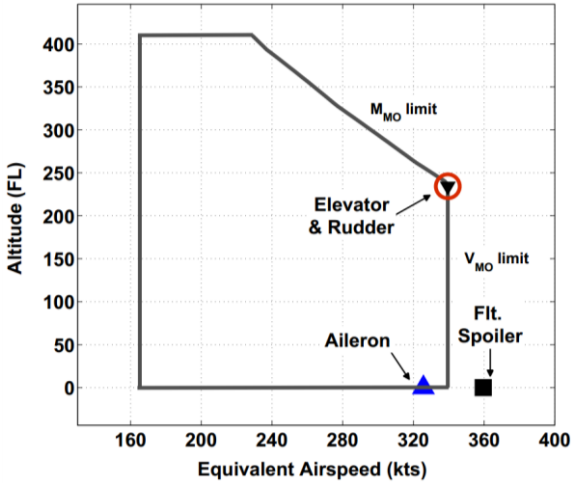

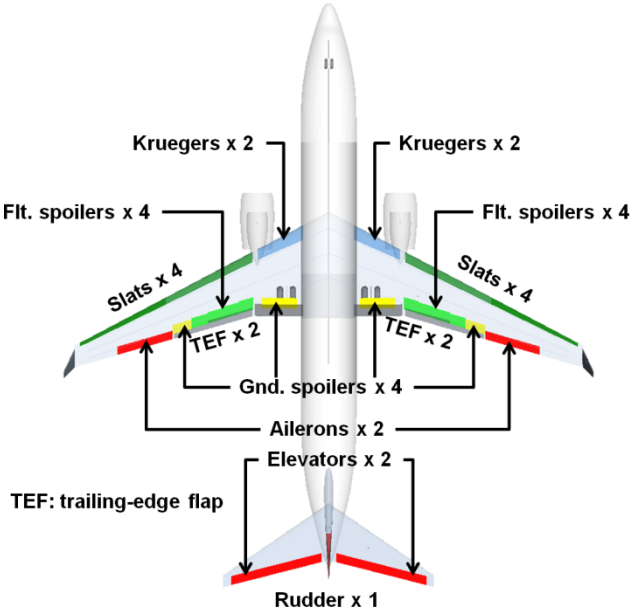

Load characteristics

- Ailerons, elevators, rudder – hinge moment coefficients [3]
- Flight & ground spoilers – hinge moment coefficients [4]
- High-lift devices – scaling wind-tunnel results [5,6]
  (or matching specifications of existing actuator)

Actuation requirements for baseline aircraft control surfaces

Control Surface	Actuating Load	Rate	#/Aircraft
Ailerons	4,200 Nm	$60°/s$	2
Elevators	7,600 Nm	$60°/s$	2
Rudder	8,200 Nm	$60°/s$	1
Flight spoilers	4,200 Nm	$60°/s$	8
Ground spoilers	3,800 Nm	$40°/s$	4
Trailing-edge flaps	51,000 N	102 mm/s	4
Leading-edge slats	6,300 N	60 mm/s	8
Krueger flaps	5,600 Nm	$16°/s$	4

Control Surface Actuation – Actuator Models

- Two types of electric actuators were modeled
  - Electrohydrostatic actuator (EHA)
  - Electromechanical actuator (EMA)

- Based on control surface actuation requirements (load, speed, stroke), actuator models were created to estimate
  - Weight [8,9]
  - power [10]

- The following association of actuators to control surfaces was considered
  - each aileron – 2 x EHA
  - each elevator – 2 x EHA
  - rudder – 3 x EHA
  - each spoiler – 1 x EHA
  - each L/E device – 1 x EHA
  - each T/E flap – 2 x EMA

- The conventional hydraulic system was not modeled in detail. Instead its weight was estimated from empirical relationships [2]

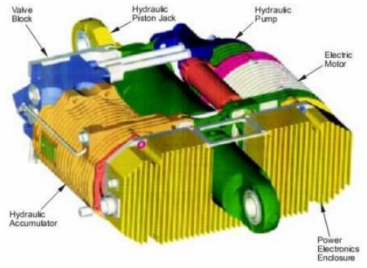

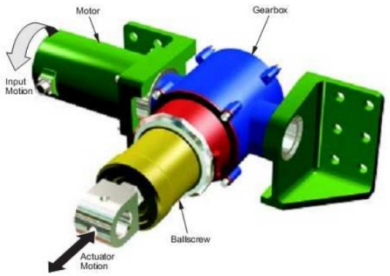

EHA **EMA**

Electrohydrostatic and Electromechanical Actuators [7]

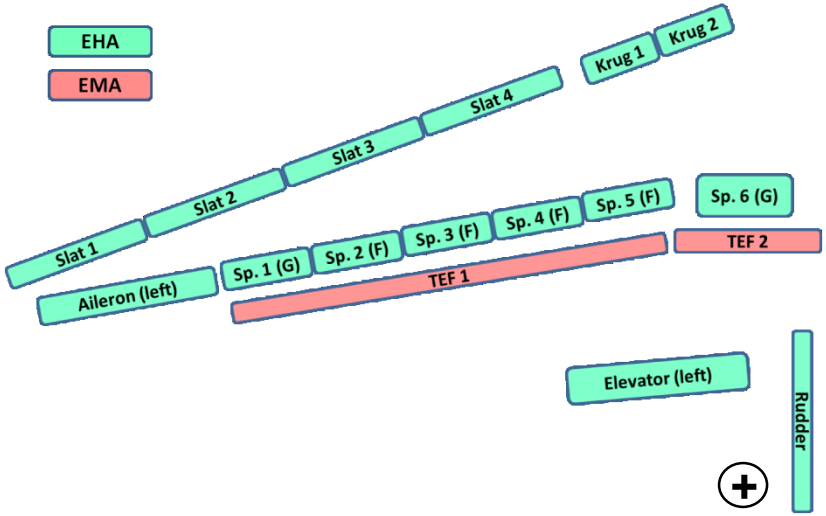

Landing Gear Actuation

- Landing gear weight was set as a fraction of the aircraft MTOW [11]
- Kinematic parameters were set based on gear leg length [12]
- Gravitational moment predominates during retraction/extension [13]
- Actuator ram position and force were obtained by solving the linkage kinematics

$$c(\theta) = \sqrt{a^2 + b^2 - 2ab\cos(\theta + \phi)},$$

$$F(\theta) = \frac{W_{lg}\ \ell_{cg}\cos\theta\ \sqrt{a^2 + b^2 - 2ab\cos(\theta + \phi)}}{\eta_m\ a\ b\ \sin(\theta + \phi)}$$

- Max force, max rate, and stroke were identified. Retraction at max actuator rate was assumed

$$F_0 = \max_{\theta \in [\theta_{up}, \theta_{dn}]} F(\theta), \qquad s = c(\theta_{dn}) - c(\theta_{up}), \qquad v_{max} = \frac{s}{\Delta t\ (1 - \epsilon)},$$

Landing gear geometry and kinematics

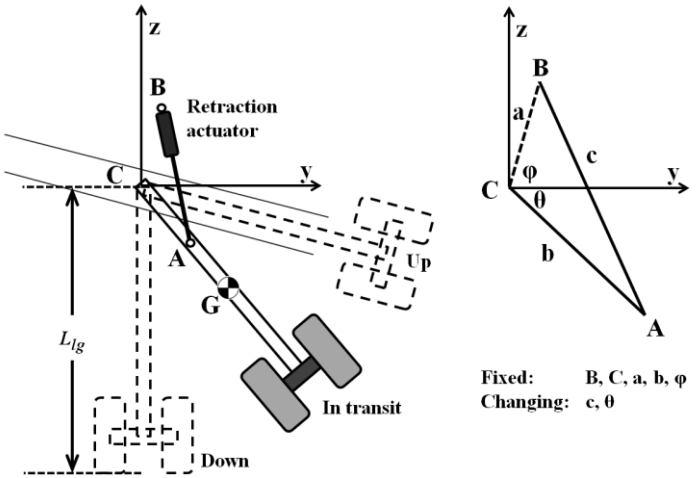

Summary of landing gear geometry & kinematic parameters

Parameter	Nose gear	Main Gear
L_{lg}	2.26 m	3.68 m
BC (a)	0.09 L_{lg}	0.09 L_{lg}
CA (b)	0.28 L_{lg}	0.28 L_{lg}
CG (ℓ_{cg})	0.5 L_{lg}	0.5 L_{lg}
ϕ	80°	80°
W_{lg}	0.5% MTOW	1.25% MTOW
η_m	0.80	0.80
θ_{up}, θ_{dn}	-20°, 90°	25°, 90°
Δt	15 sec	15 sec

Wheel Braking

- Braking force requirements were obtained by considering 2 static cases [14] & 2 dynamic cases [15]

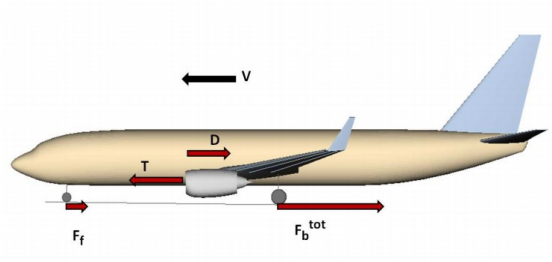

Case description	Full-throttle run-up	Parking on incline	Accelerate-stop	Landing decel.
Case type	Static (S1)	Static (S2)	Dynamic (D1)	Dynamic (D2)
Aircraft weight	MTOW	MRW	MTOW	MLW
Thrust setting	Max. SLS	-	Idle	Idle
Ground speed	-	-	72 m/s (140 kts)	75 m/s (145 kts)
Deceleration	-	-	1.8 m/s^2(6.0 ft/s^2)	3.0 m/s^2(10 ft/s^2)
Opposing gradient	1.1°	1.1°	1.1°	1.1°

$$F_b^{tot} = T - D - F_f + W\sin\theta - \frac{W}{g}\frac{dV}{dt}, \qquad F_b = \frac{F_b^{tot}}{n_{brk}}.$$

- Braking force → Braking torque → Axial force

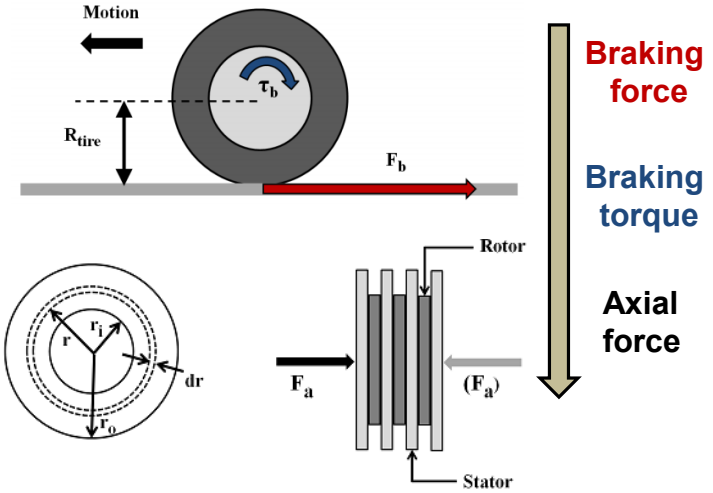

- Brake "heat-stack" mass was computed based on thermal capacity required to dissipate the kinetic energy (KE) within a permissible *gross* temperature rise

$$\Delta KE = m_{hs}\ c\ \Delta T_{max}$$

- Weight predictions obtained were in fair agreement with published weights for steel and carbon-carbon brakes [16,17]

- For the electric brake, the mass of the EMA was added to the mass of the heat-stack

Parameter	Steel (CSA)	C-C (ESA)
Specific Heat (c)	544.3 J/kg/K	1297.9 J/kg/K
Permissible temp. rise (ΔT_{max})	500° C	500° C
Friction coefficient (μ)	0.3	0.3
Dissipated kinetic energy (ΔKE)	max. of D1 & D2	max. of D1 & D2

Nose-wheel Steering

- Nose landing gear parameters were set based on conceptual design phase guidelines [1]
- The conditions cited in FAR 25.499 (Nose-wheel yaw and steering) were used to estimate the moment about the steering axis
  - Aircraft at Maximum Ramp Weight (MRW)
  - Vertical force equal to 1.33 times the maximum nose gear static reaction
  - Nose gear side (lateral) force of 0.8 times the vertical ground reaction
- The steering moment was computed from the tire lateral force using the steering geometry

$$M_{max}^{nws} = L_{eff}\ F_{y,max}^{nlg} = L_{eff} \left(\frac{F_y^{nlg}}{F_z^{nlg}}\right) F_{z,max}^{nlg} = (x_{tire}\ \cos\theta_r) \left(\frac{F_y^{nlg}}{F_z^{nlg}}\right) (\kappa\ \epsilon_s\ MRW)$$

- Predicted steering moment showed good agreement with results from ELGEAR project (A320) [18]

NLG parameters	Symbol	Values
Max. static load	ϵ_s	15 %
Rake angle	θ_r	7°
Tire radius	r_{tire}	38 cm
Tire trail	x_{tire}	18 % of tire radius
NWS parameters	**Symbol**	**Values**
Deflection	$\delta_{max}, \delta_{min}$	± 75°
Rate	$\omega_{max}, \omega_{min}$	± 20°/s

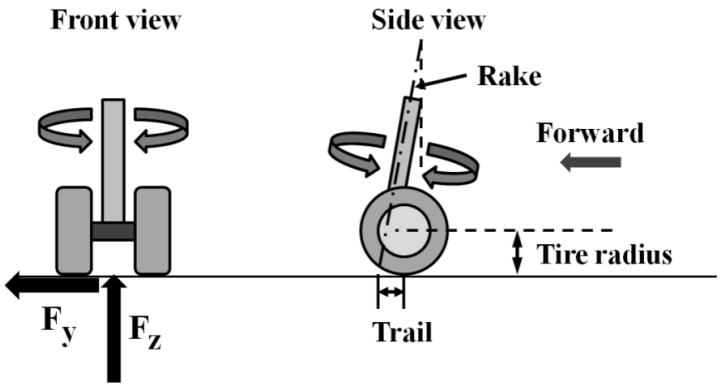

Environmental Control System – Cabin Air Requirements

- Cabin was considered divided into thermal zone each with independent temperature setting

- Thermal loads considered:
  - Passenger metabolic heat load
  - Galley loads, Electrical/electronic heat loads
  - Heat exchange with ambient through cabin wall

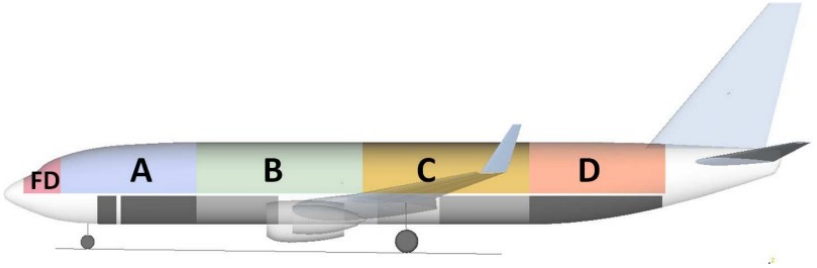

Thermal zones considered for ECS cabin model

- Minimum mass flow rate was set

$$\begin{aligned} \dot{m}_i^{min} &= \frac{V_{zone}}{\Delta t_{cycle}}, && \text{(based on air cycle time)} \\ &= \rho_{air}\ \dot{V}_{\text{per pax}}\ n_{\text{pax}}, && \text{(based on volume flow rate per occupant)} \end{aligned}$$

- Zone thermal load and inlet temperature constraints were used to determine
  - Required mass flow rate
  - Required inlet temperature

$$\begin{aligned} \dot{Q}_i &= \dot{m}_i^{min}\ C_{p,air}\ (\tilde{T}_{in,i} - T_i), && \text{(solve for } \tilde{T}_{in,i}) \\ T_{in,i} &= \min\left(T_{in,i}^{max}, \max\left(T_{in,i}^{min}, \tilde{T}_{in,i}\right)\right), && \text{(respect inlet temperature constraints)} \\ \dot{m}_i &= \frac{\dot{Q}_i}{C_{p,air}\ (T_{in,i} - T_i)}. && \text{(compute required mass flow rate)} \end{aligned}$$

Environmental Control System – Air Distribution & Recirculation

- Return air from cabin zones enters mixing manifold (for recirculation)
- 50% recirculation was assumed
- Fresh (conditioned) pack air received from two ECS packs
- Each ECS pack was supplied by 2 cabin air compressors (CACs)
- Cabin zone with lowest inlet temperature requirement sets the output temperature from the mix manifold
- The temperature requirements of the remaining zones are satisfied using “trim” air (hot air that bypasses the ACMs)

$$\dot{m}_{trim,i} = \frac{\dot{Q}_i - \dot{m}_i \, C_{p,air} \, (T_s - T_i)}{C_{p,air} \, (T_{trim} - T_i)}$$

- Source of fresh cabin air
  - ***Electric ECS:*** external ram air compressed by CACs
  - ***Conventional ECS:*** engine bleed air

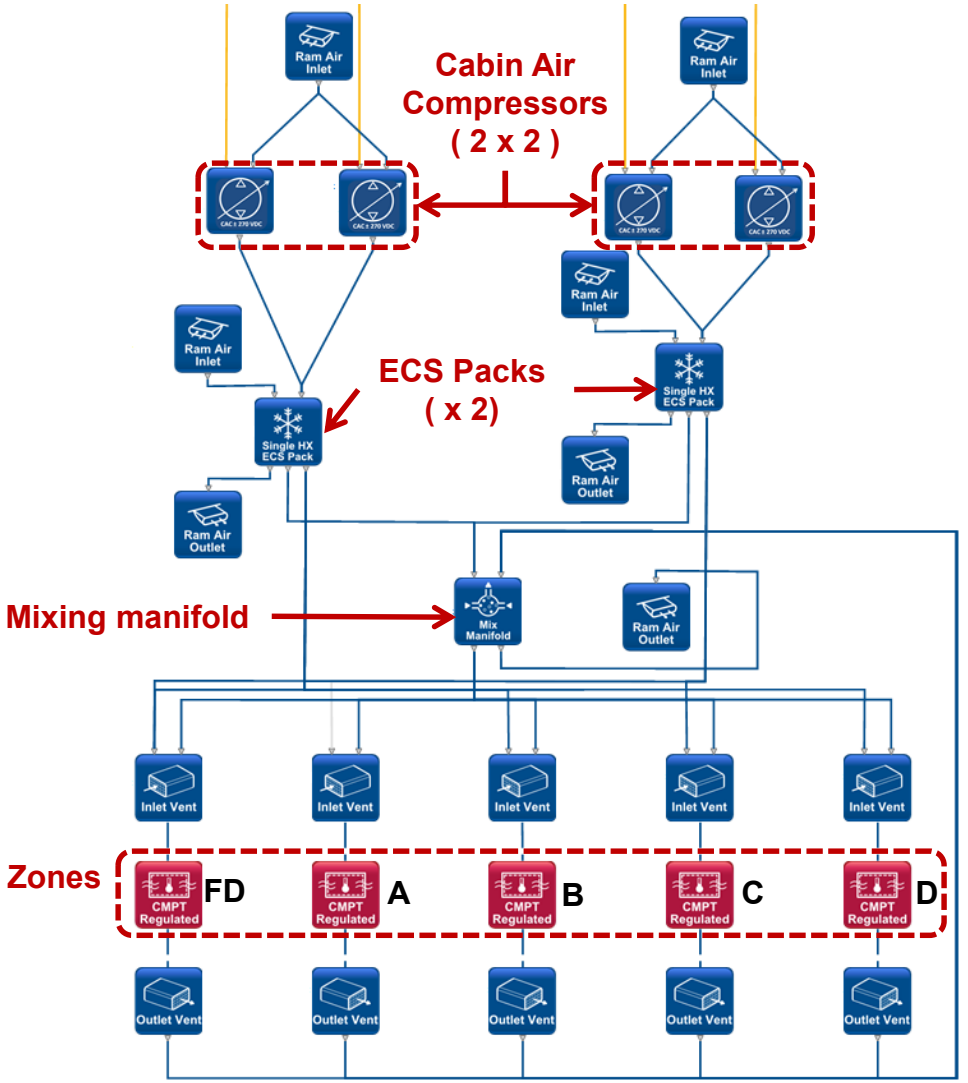

Ice Protection System – Computation of Required Heat Flux

- Protected areas
  - Slats 2, 3, 4, 5, 6, 7
  - Engine nacelle inlets
- Required heat flux depends on ambient conditions and also the target skin temperature
  - Evaporative systems: 37 – 50 °C
  - Running-wet systems: 4 – 10 °C
- Surface heat flux is the resultant of heat fluxes from five processes [19,20]:
  - Convection
  - Sensible heating
  - Evaporation
  - Kinetic heating
  - Aerodynamic heating

$$\dot{q}_{tot} = \dot{q}_{conv} + \dot{q}_{sens} + \dot{q}_{evap} + \dot{q}_{kin} + \dot{q}_{aero}$$

$$\begin{aligned} \dot{q}_{conv} &= h_0(T_{skin} - T_\infty), \qquad h_0 = \frac{Nu\ k_0}{x} \\ Nu &= 0.0296\ Re^{4/5}\ Pr^{1/3}, \quad Re = \frac{\rho V_\infty x}{\mu}, \quad Pr = \frac{\mu C_p}{k_0} \end{aligned}$$

$$\begin{aligned} \dot{q}_{sens} &= \dot{m}_{local}\left(\Delta T\left((1-n)\ c_w + n\ c_i\right) + n\ L_f\right) \\ \Delta T &= T_{skin} - T_\infty, \qquad n = \frac{c_w(T_{ref} - T_\infty)}{L_f}, \end{aligned}$$

$$\dot{q}_{evap} = \min\left(\dot{m}_{local} L_e,\ -0.7\ h_0\ L_e\ \frac{R_h\ e_\infty - e_{skin}}{p_\infty C_p}\right)$$

$$\begin{aligned} \dot{q}_{kin} &= -\dot{m}_{local}\frac{v_\infty^2}{2} \\ \dot{q}_{aero} &= -R_c\ h_0\ \left(\frac{\gamma - 1}{2}\right)\ M_\infty^2\ T_\infty \\ R_c &= 1 - 0.99\ (1 - Pr^{0.5}), \end{aligned}$$

$$\dot{m}_{local} = v_\infty\ \rho_{LWC}\ E_m, \qquad E_m = 0.00324\ \left(\frac{v_\infty}{t}\right)^2,$$

Ice Protection System – Pneumatic & Electrothermal

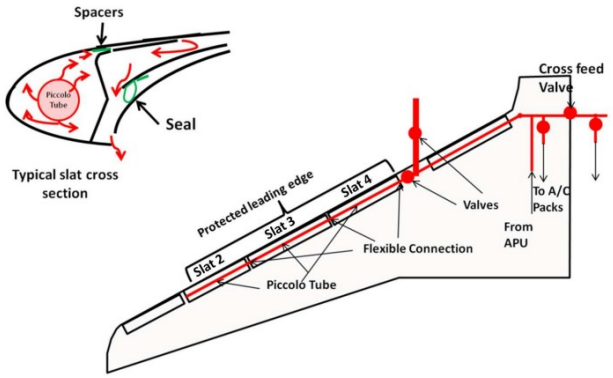

Pneumatic IPS

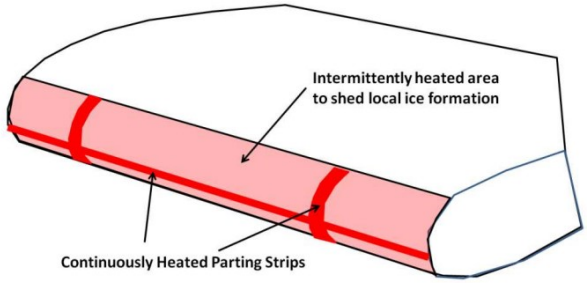

Electrothermal IPS [21]

$$
\begin{aligned}
T_{wall} &= T_{skin} + \frac{\dot{q}_{tot}\ t_{skin}}{k_{skin}} \approx T_{skin} \\
\bar{T}_{bay} &= T_{wall} + \frac{\dot{q}_{tot}}{h_{int}} \\
\dot{m}_{bleed} &= \frac{\dot{q}_{tot}\ A_{prot}}{C_{p,air}\ (T_{supply} - \bar{T}_{bay})}
\end{aligned}
$$

$$
\begin{aligned}
\dot{q}_{cyc} &= \frac{m_{ice}}{t_{heat}}\ \left(c_i\ (T_{ref} - T_\infty) + L_f\right), \\
\dot{q}_{eff} &= \dot{q}_{ps}\ \kappa_{ps} + \dot{q}_{cyc}\ (1 - \kappa_{ps})\ \kappa_{cyc}, \\
P_{req} &= \frac{A_{prot}\ \dot{q}_{eff}}{\eta_{heat}},
\end{aligned}
$$

Parameter	Symbol	Values
Parting strip area ratio	κ_{ps}	20 %
Cyclic heating activity ratio	κ_{cyc}	5 %
Heat "on" time	t_{heat}	9 sec
Ice thickness to melt	ℓ_{ice}	0.5 mm
Protected area / wing	A_{prot}	3.45 m^2
Protected area / nacelle	"	4.01 m^2
Overall heater efficiency	η_{heat}	70 %

Electric Taxiing

- Electric motors were assumed to be driving the main gear axles (as opposed to nose gear)
- Main requirements are acceleration, max taxiing speed, and achieving breakaway torque

Scenario	Initial speed	Final speed	Time interval	Gradient	Loadout
Acc. to max taxi speed	0 kt	18 kt	90 sec	-	MTOW
Acc. for runway crossing	0 kt	10 kt	20 sec	-	MTOW
Maintain max taxi speed	-	20 kt	-	-	MTOW
Achieve breakaway	0 kt	-	-	1.5 %	MRW

- A linearly-reducing acceleration profile was assumed to compute velocity as a function of time

$$a_{max} = \frac{2\Delta v}{\Delta t}, \qquad a(t) = a_{max}\left(1 - \frac{t}{\Delta t}\right) \implies v(t) = v(0) + a_{max}t - \frac{a_{max}}{2\Delta t}\,t^2$$

- The required tractive force per tire was used to compute max torque and power requirement

$$F_d = \frac{1}{2}\left(F_f + m\frac{dV}{dt}\right) \qquad \tau_m(t) = \frac{F_d(t)\; r_{tire}}{\eta_m},$$

$$P_m(t) = \tau_m(t)\;\omega_{tire}(t) = \frac{\tau_m(t)\;v(t)}{r_{tire}},$$

$$\tau_{m,max} = \max_{t\in[0,\Delta t]} \tau_m(t), \qquad P_{m,max} = \max_{t\in[0,\Delta t]} P_m(t),$$

- Predicted motor power compared well with published figure from Airbus/Honeywell/Safran ***"Electric Green Taxiing System"*** (EGTS) test program (2 x 50 kW, A320 aircraft) [22]

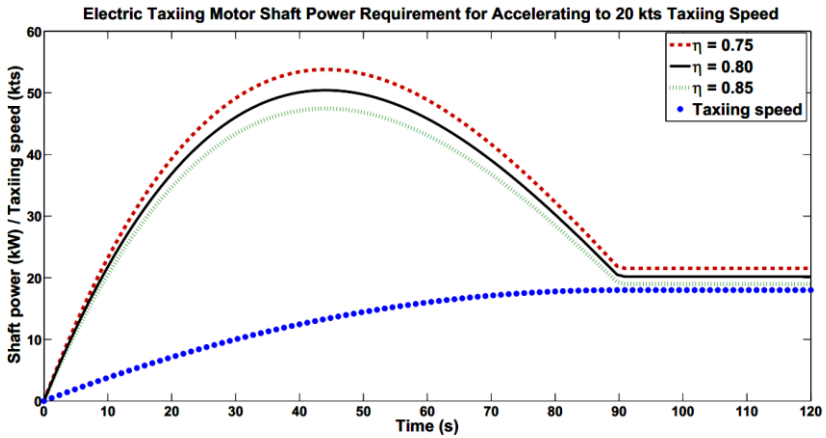

Figure 9. Shaft power requirement (kW) for each of two electric taxiing motors for acceleration to 18 kts taxiing speed in 90 seconds. Aircraft MTOW is 79,000 kg. Rolling friction coefficient 0.03. Nose landing gear weight fraction 15 %. Efficiencies are for power transmission downstream of motor output shaft.

Agenda

- Introduction and Motivation
- Subsystems
- Implementation and Architecture Application
- Summary

Integration of Methods & Models into Pacelab SysArc Environment

Actuation subsystems + Electric Taxiing

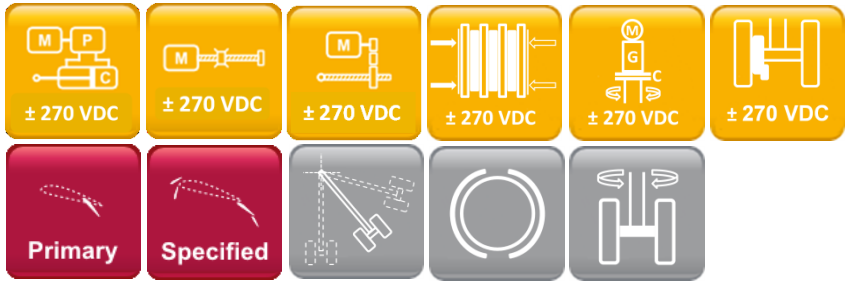

Environmental Control System (ECS)

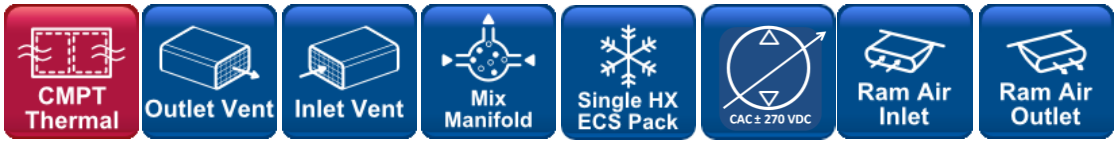

Ice Protection System (IPS)

- Subsystem component models, methods, etc. were incorporated into Pacelab SysArc "Engineering Objects" (EO's)
- Several existing EO's were used, with modifications made where necessary
- No detailed model of conventional centralized hydraulic architecture was created

Power Generation and Distribution

- The Electric Subsystem Architecture (ESA) was built around the Power Generation & Distribution system
- Partly based on the architecture of the Boeing 787 [24,25]
- Sizing of generators based power consumption of flight-critical systems during One Engine Inoperative (OEI) flight
- APU sizing driven by ECS operation on ground
- Electric loads (e.g. control surface actuators) were connected to electric busses in a manner similar to association of hydraulic actuators to redundant hydraulic systems

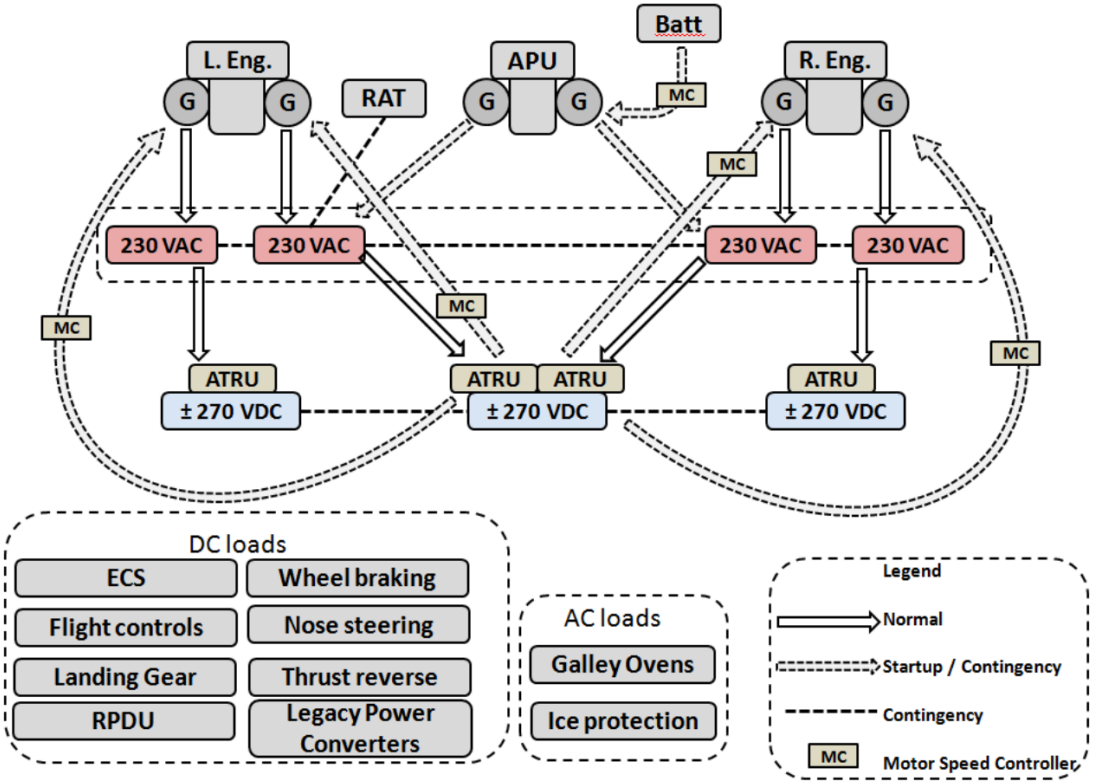

Subsystem Architecture in Pacelab SysArc – Logical Connections

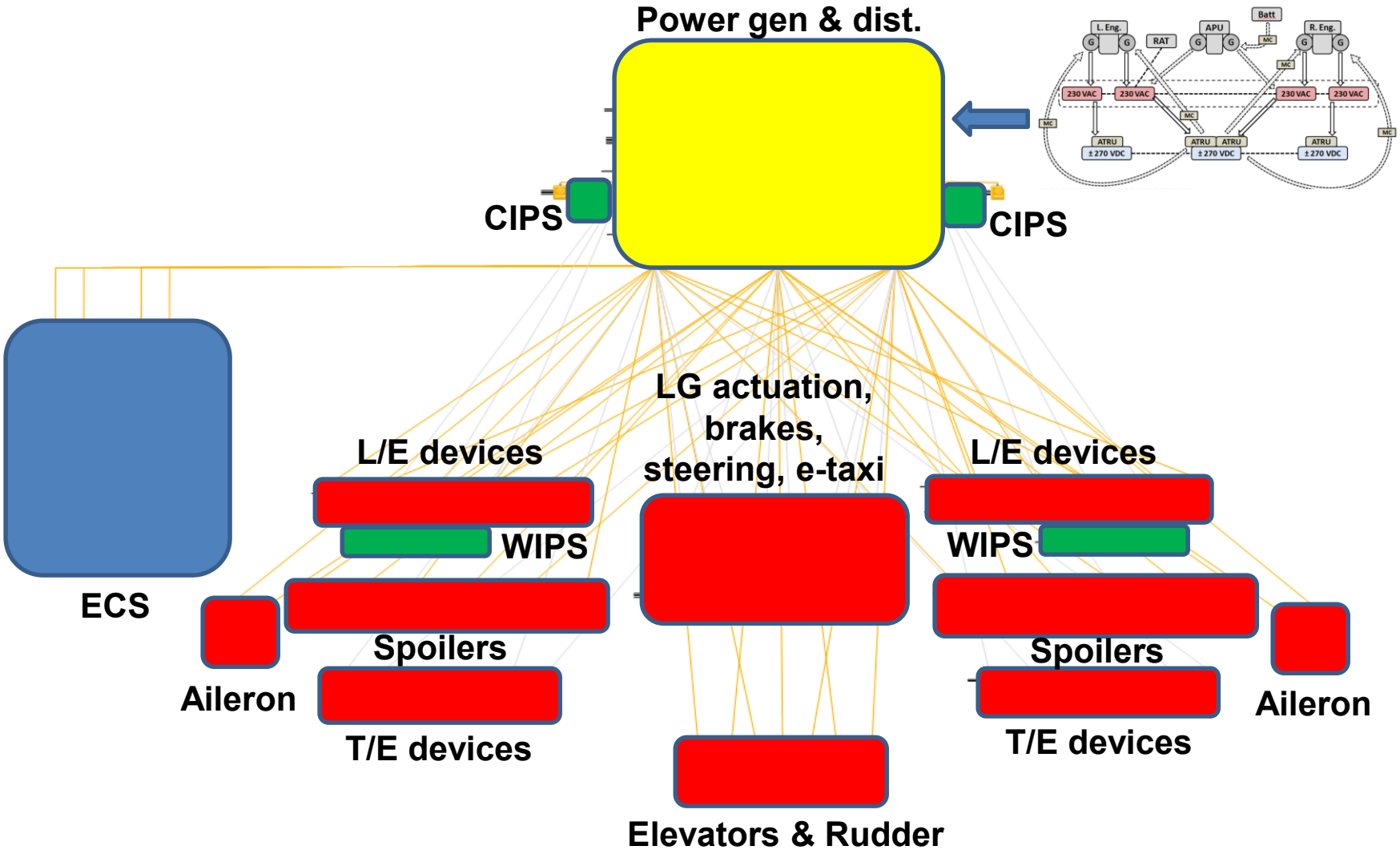

Subsystem Architecting in Pacelab SysArc – Physical Connections

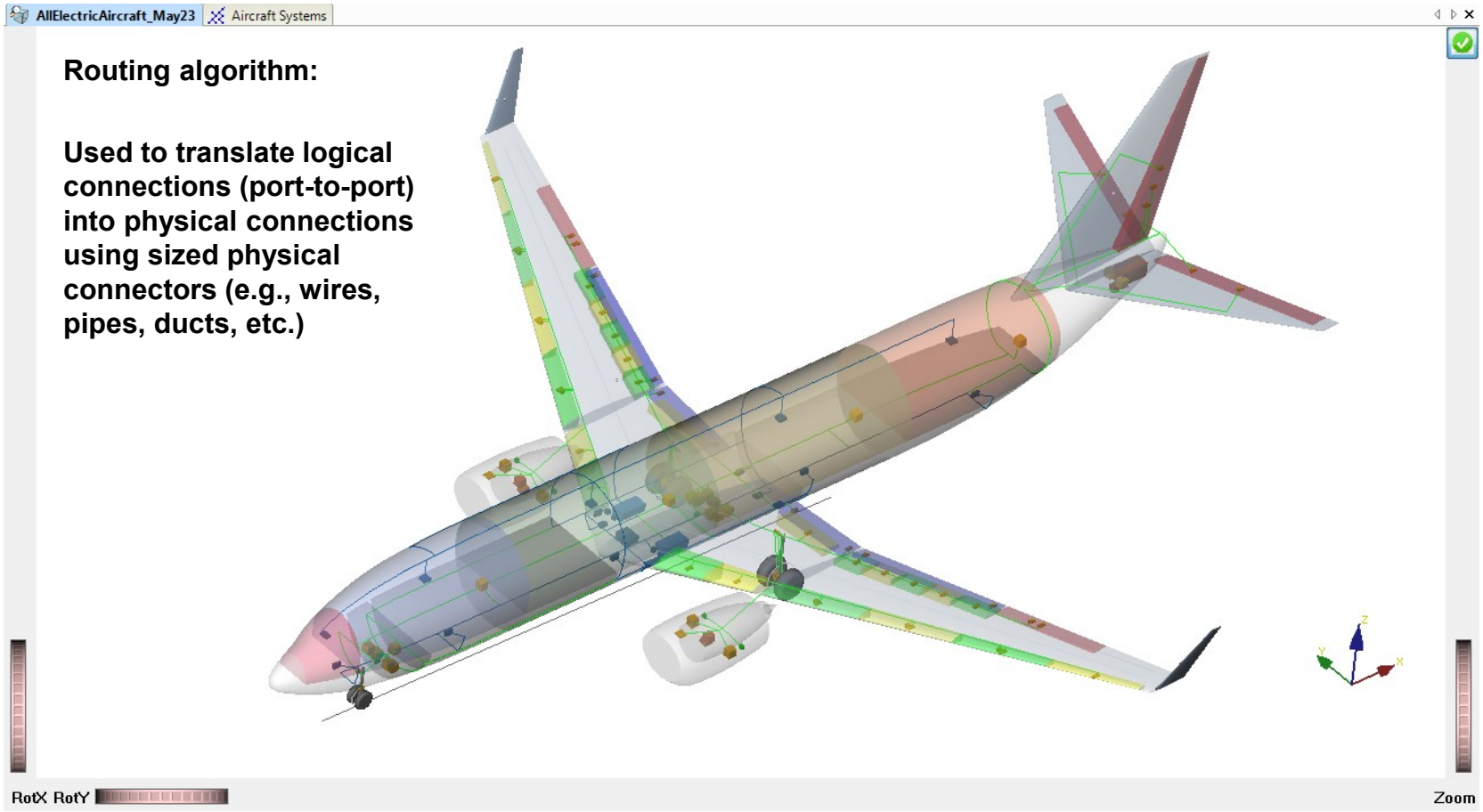

Estimating Change in Aircraft Operating Empty Weight (OEW)

- Empirical relationships were used to estimate Δweight due to deletion of hydraulic & pneumatic systems
- Power-to-weight ratios of generators, APU, & ATRU were based on public domain information
- Electric taxiing system was not considered further (more likely to be a retro-fit for short haul operations)
- Change in fixed equipment
  → change in vehicle OEW
  → change in required fuel
  → change in vehicle MTOW

Deletions	Additions	Δ Mass (kg)	
Hydraulics & pneumatics		−540	
Conventional surface controls		−1,451	
	Electric CS & LG actuators		+ 996
Conventional brakes (x 4)		−760	
	EMA brakes (x 4)		+ 582
	Electric nose-wheel steering		+ 79
Pneumatic WIPS & CIPS		−61	
	Electrothermal WIPS & CIPS		+ 95
	ECS Cabin Air Compressors (x 4) (50 kW each, 2.5 kW/kg)		+ 80
2 x 120 kVA generators (2.76 kVA/kg)		−87	
	4 x 135 kVA generators (2.76 kVA/kg)		+ 196
	Additional wiring/cabling		+ 84
	ATRU (x 4)		+ 130
	Higher capacity APU (from 100 kW to 280 kW, 1.83 kW/kg)		+ 98
Net fixed equipment Δ Mass : − 560 kg (− 1,232 lb) ←		−2,899	+ 2,339

Mission Definition and Engine Performance Tables

- Engine decks for mission performance analysis were generated using the Numerical Propulsion System Simulation (NPSS) tool [27], which was used to generate *two* engine decks
  - for CSA-design: shaft-power extraction + bleed (i.e, mixed off-take)
  - for ESA-design: only shaft-power extraction

- Engine decks were representative of the CFM56-7B27 engine [28], but did not utilize or contain any proprietary information

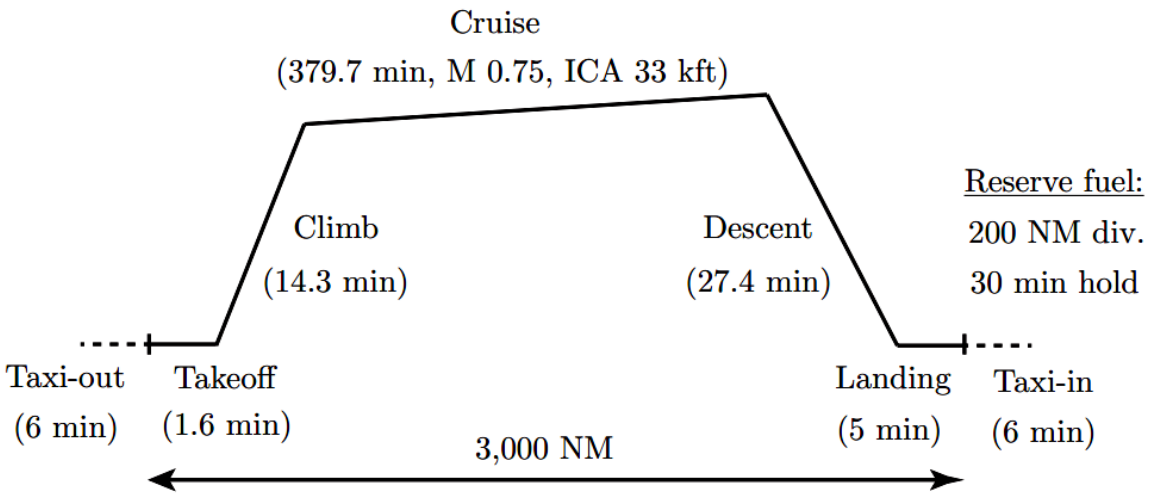

Subsystem Activity Schedules

- Control surface movements were characterized by amplitude and frequency for each flight phase
- Figures for cruise are representative of a turbulence encounter
- Common loads were scaled from previous AEA studies
- For both architectures, 50% ECS recirculation was assumed
- IPS set to “OFF” in cruise for both designs

Surface →	Aileron		Elevator		Rudder		Flt. Spoiler	
Phase ↓	$+\bar{\delta}/-\bar{\delta}$	f (Hz)	$+\bar{\delta}/-\bar{\delta}$	f (Hz)	$+\bar{\delta}/-\bar{\delta}$	f (Hz)	$\bar{\delta}$	f (Hz)
Ground	+1/-1	0.4	+1/-1	0.4	+1/-1	0.4	1	0.4
Takeoff	+0.12/-0.2	0.4	+0.2/-0.2	0.4	+0.2/-0.2	0.4	0.12	0.4
Climb	+0.12/-0.2	0.2	+0.2/-0.2	0.2	+0.2/-0.2	0.2	0.12	0.2
Cruise	+0.5/-0.5	0.4	+0.3/-0.3	0.4	+0.3/-0.3	0.4	0.5	0.4
Descent	+0.12/-0.2	0.3	+0.2/-0.2	0.3	+0.2/-0.2	0.3	0.12	0.3
Landing	+0.4/-0.53	0.3	+0.53/-0.53	0.3	+0.53/-0.53	0.3	0.4	0.3

CDA & AEA	Unit	Ground	Takeoff	Climb	Cruise	Descent	Landing
Instruments	kW	8	8	8	8	8	8
In-flight entertainment	kW	10	10	10	10	10	10
Galley loads	kW	0	0	40	40	0	0
Essential lighting	kW	10	10	10	10	10	10
Engine-driven fuel pump	kW	8	8	8	8	8	8
Electric fuel pump	kW	8	8	8	8	8	8
ECS recirculation	kW	5	5	5	5	5	5
E/E cooling	kW	6	6	6	6	6	6
Miscellaneous loads	kW	5	5	5	5	5	5
+ Only CDA	**Unit**	**Ground**	**Takeoff**	**Climb**	**Cruise**	**Descent**	**Landing**
Hydraulic system	kW	0	14	22	21	22	19
ECS	kg/s	1.05	1.05	1.05	1.05	1.05	1.05
Wing IPS (running-wet)	kg/s	0.97	0.97	0.2	0	0.31	0.97
Nacelle IPS (evaporative)	kg/s	1.13	1.13	2.58	0	1.09	1.13

Propagating Effect of CSA-to-ESA Architecture Transition

Baseline

CSA

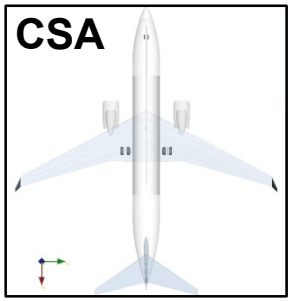

S_w (sq.ft.)	1,343
W/S (psf)	127.5
SLST (lbf)	54,600
T/W	0.3189
OEW (lb)	92,310
MTOW (lb)	171,200
Fuel (lb)	38,704

CSA: Conventional Subsystems Architecture

CSA→ESA

Hold… OEW, geometry, thrust

Intermediate

ESA-I

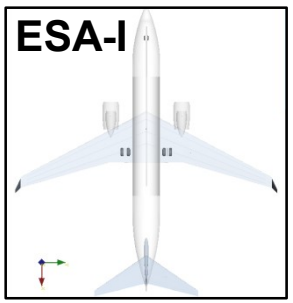

Δ S_w	-
Δ W/S	- 0.88 %
Δ SLST	-
Δ T/W	+ 0.88 %
Δ OEW	-
Δ MTOW	- 0.88 %
Δ Fuel	- 3.50 %

- Isolates the effect of transitioning from mixed off-take to "bleedless"
- Shows that it is possible to absorb some amount of OEW increase

Factor in Δ OEW

Hold… geometry, thrust

Uncycled

ESA-U

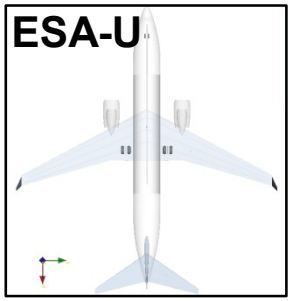

Δ S_w	-
Δ W/S	- 1.98 %
Δ SLST	-
Δ T/W	+ 2.02 %
Δ OEW	- 1.69 %
Δ MTOW	- 1.98 %
Δ Fuel	- 4.20 %

- Isolates the effect of CSA→ESA with fixed propulsor & geometry
- Shows that increased range and/or payload capability is possible

Resize vehicle & propulsor

Cycled

ESA-C

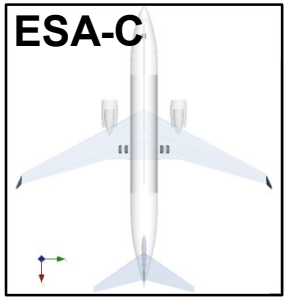

Δ S_w	- 2.92 %
Δ W/S	-
Δ SLST	- 2.92 %
Δ T/W	-
Δ OEW	- 2.97 %
Δ MTOW	- 2.92 %
Δ Fuel	- 5.12 %

- Captures the additional "snowball" effect by "cycling" the design
- Iteration affects vehicle, propulsor, *and* subsystems

ESA: Electric Subsystems Architecture

Agenda

- Introduction and Motivation
- Subsystems
- Implementation and Architecture Application
- Summary

Conclusions & Future Work

Conclusions:

- Subsystem sizing and analysis methods suitable for the conceptual aircraft design phase were developed / identified for major aircraft subsystems
  - Actuation subsystems (flight controls, landing gear, brakes, steering)
  - Environmental control system (ECS)
  - Ice protection system (IPS)

- These methods were integrated into an environment (Pacelab SysArc) that allowed the propagation of subsystem effects on the aircraft and its mission performance to be analyzed

- A proposed methodology to integrate the sizing and analysis of subsystems into aircraft conceptual design was demonstrated by considering the vehicle and mission level effects of transitioning from conventional to electric subsystem architecture

Future work:

- Enhance the physics modeling in the analysis methods used
- Consider additional subsystems (e.g., thrust reversers, etc.)
- Consider the effect of electric subsystems on different *categories* of aircraft: (general aviation, business jets, commercial transports of varying size)

References

1. Raymer, D., Aircraft Design: A Conceptual Approach, AIAA Education Series, 4th ed.
2. Roskam, J., Airplane Design Part V - Component Weight Estimation, Design Analysis & Research, 1999.
3. Roskam, J., Airplane Design Part VI - Preliminary Calculation of Aerodynamic, Thrust and Power Characteristics, Design Analysis & Research, 1999.
4. Scholz, D., "Development of a CAE-Tool for the Design of Flight Control and Hydraulic Systems," in "AeroTech '95, Birmingham," 1995.
5. Kelly, J. and McCullough, G., "Aerodynamic Loads on a Leading-edge Flap and a Leading-edge Slat on the NACA 64A010 Airfoil Section (NACA TN 3220)," Tech. rep., National Advisory Committee for Aeronautics (NACA), 1954.
6. Moraris, V., Lawson, N., and Garry, K., "Aerodynamic and Performance Characteristics of a Passive Leading Edge Krueger Flap at Low Reynolds Numbers," The Aeronautical Journal, Vol. 116 (1181), 2012, pp. 759–769.
7. Botten, S., Whitley, C., and King, A., "Flight Control Actuation Technology for Next-Generation All-Electric Aircraft," Technology Review Journal - Millenium Issue, pp. 55–68.
8. Chakraborty, I., Jackson, D., Trawick, D., and Mavris, D., "Development of a Sizing and Analysis Tool for Electrohydrostatic and Electromechanical Actuators for the More Electric Aircraft," in "AIAA Aviation 2013 Conference," Los Angeles, California, AIAA 2013-4282, 2013.
9. Chakraborty, I., Trawick, D., Jackson, D., and Mavris, D., "Electric Control surface Actuator Design Optimization and Allocation for the More Electric Aircraft," in "AIAA Aviation 2013 Conference," Los Angeles, California, AIAA 2013-4283, 2013.
10. Chakraborty, I., Mavris, D., Emeneth, M., and Schneegans, A., "A System and Mission Level Analysis of Electrically Actuated Flight Control Surfaces using Pacelab SysArc," in "AIAA Science and Technology Forum and Exposition (SciTech 2014)," National Harbor, MD, AIAA-2014-0381, 2014.
11. Jenkins, S., "Landing Gear Design and Development," in "Proceedings of the Institution of Mechanical Engineers Part G - Journal of Aerospace Engineering," Vol. 203, 1989, pp. 67–73.
12. Young, D., "Aircraft landing gears - the past, present and future," Proceedings of the Institution of Mechanical Engineers, Part D: Journal of Automobile Engineering, Vol. 200, No. 2, 1986, pp. 75–92.
13. Li, W. and Fielding, J., "Preliminary Study of EMA Landing Gear Actuation," in "28th International Congress of the Aeronautical Sciences (ICAS 2012)," 2012.
14. Collins, A., "EABSYS: Electrically Actuated Braking System," in "IEE Colloquium. Electrical Machines and Systems for the More Electric Aircraft," , 1999, p. 4.
15. "Federal Aviation Regulations (FAR) Part 25 - Airworthiness Standards: Transport Category Airplanes, Federal Aviation Administration (FAA)," available online at http://www.ecfr.gov/.
16. Allen, T., Miller, T., and Preston, E., "Operational Advantages of Carbon Brakes," Online: www.boeing.com/commercial/Aeromagazine, 2009 Quarter 3.

References

17. Honeywell, “Boeing 737 NG Wheel and CERAMETALIX Brake - Proven braking performance and reliability with low operational costs,” http://aerospace.honeywell.com/~/media/UWSAero/common/documents/myaerospacecatalog-documents/ATR_Brochures-documents/737NG_Data_Sheet_US.pdf.
18. Bennett, J., Mecrow, B., Atkinson, D., Maxwell, C., and Benarous, M., “Fault-tolerant electric drive for an aircraft nose wheel steering actuator,” IET Electrical Systems in Transportation, Vol. 1, No. 3, 2011, pp. 117–125.
19. Al-Khalil, K., Horvath, C., Miller, D., and Wright, W., “Validation of Thermal Ice Protection Computer Codes: Part 3 - The Validation of ANTICE,” in “35th Aerospace Sciences Meeting and Exhibit,” AIAA-97-0051, 1997.
20. Meier, O. and Scholz, D., “A Handbook Method for the Estimation of Power Requirements for Electrical De-Icing Systems,” in “DLRK, Hamburg,” 2010.
21. Krammer, P. and Scholz, D., “Estimation of Electrical Power Required for Deicing Systems,” Tech. rep., Aircraft Design and Systems Group, Department of Automotive and Aeronautical Engineering, Hamburg University of Applied Sciences (HAW), 2009.
22. Nicolas, Y., “eTaxi - Taxiing aircraft with engines stopped,” Flight Airworthiness Support Technology (FAST) 51, Airbus Technical Magazine, http://www.airbus.com/support/publications/, 2013.
23. Chakraborty, I., Mavris, D.N., Emeneth, E., and Schneegans, A., "A Methodology for Vehicle and Mission Level Comparison of More Electric Aircraft Subsystem Solutions - Application to the Flight Control Actuation System", Proceedings of the Institution of Mechanical Engineers, Part G: Journal of Aerospace Engineering (accepted for publication, June 2014)
24. Sinnett, M., “Boeing 787 No-Bleed Systems: Saving Fuel and Enhancing Operational Efficiencies,” www.boeing.com/commercial/aeromagazine, 2007.
25. Nelson, T., “787 Systems and Performance,” Online: http://dibley.eu.com/documents/B787SystemsandPerf-GeorgeBeyle-31mar09.pdf, 2009.
26. Kirby, M. and Mavris, D., “The Environmental Design Space,” in “26th International Congress of the Aeronautical Sciences (ICAS),” Anchorage, Alaska, 2008.
27. “Numerical Propulsion System Simulation (NPSS): An Award Winning Propulsion System Simulation Tool,” Online: https://www.grc.nasa.gov/WWW/RT/RT2001/9000/9400naiman.html.
28. CFM56-7BE For the Boeing 737 Family,” Online: http://www.cfmaeroengines.com/files/brochures/cfm56-7b.pdf.

Supplementary Information

Comparison of Predicted H.M. with F-18 SRA Flight Test H.M.

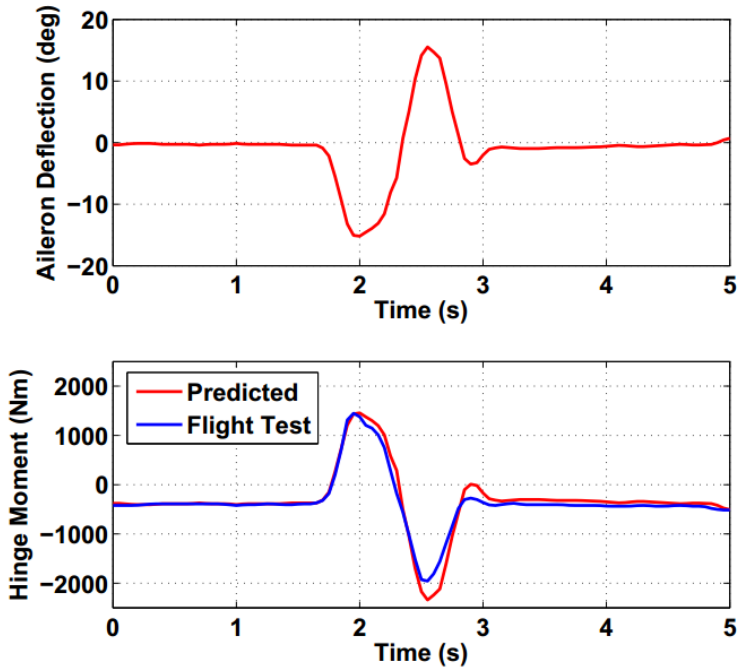

(a) Abrupt roll doublet - full stick (left): M = 0.72, h = 25 kft, q-bar = 13.60 kPa (284 lbf/sq.ft.)

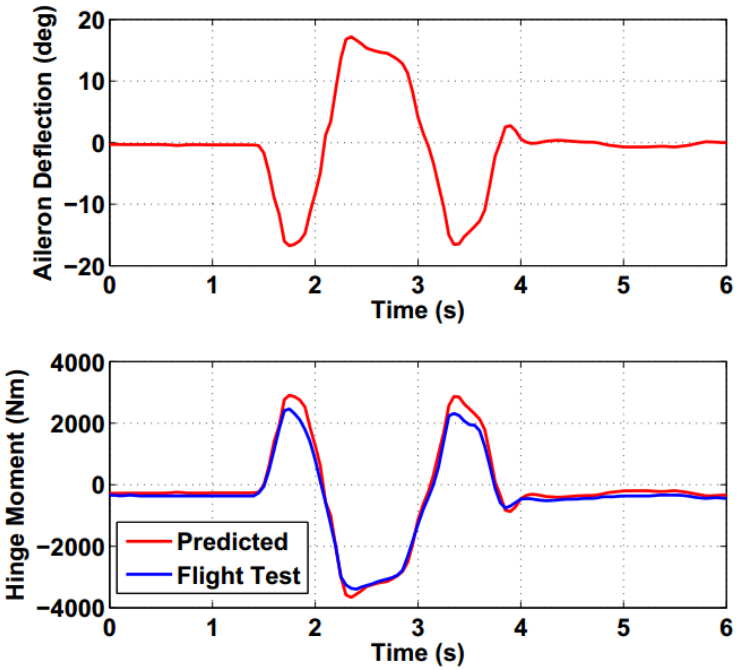

(b) Abrupt aileron reversal - full stick (left): M = 0.84, h = 25 kft, q-bar = 18.29 kPa (382 lbf/sq.ft.)

Chakraborty, I., Trawick, D., Hegde, C., Choi, H., Mendez-Ramos, E., Mavris, D.N., ***"Development of a Modeling and Simulation Environment for Real-time Performance Analysis of Electric Actuators for Maneuvering Flight"***, 51st AIAA Aerospace Sciences Meeting Including The New Horizons Forum and Aerospace Exposition, Grapevine, TX, January 7-10, 2013, AIAA-2013-0471

Hegde, C., Chakraborty, I., Trawick, D., Choi, H., Mendez-Ramos, E., Mavris, D.N., ***"A Surrogate Model Based Constrained Optimization Architecture for the Optimal Design of Electrohydrostatic Actuators for Aircraft Flight Control Surfaces"***, 51st AIAA Aerospace Sciences Meeting Including The New Horizons Forum and Aerospace Exposition, Grapevine, TX, January 7-10, 2013, AIAA-2013-0470

Control Surface Definition in Pacelab SysArc

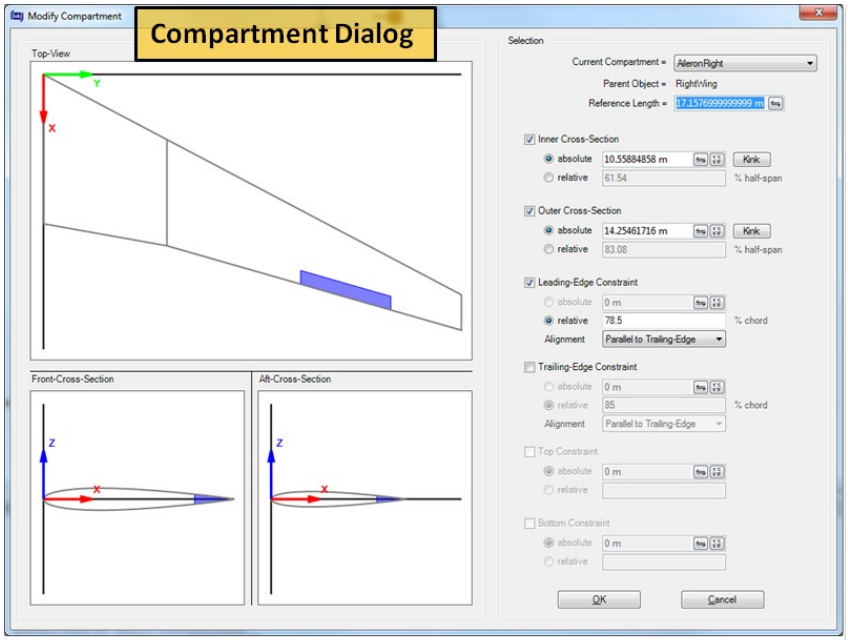

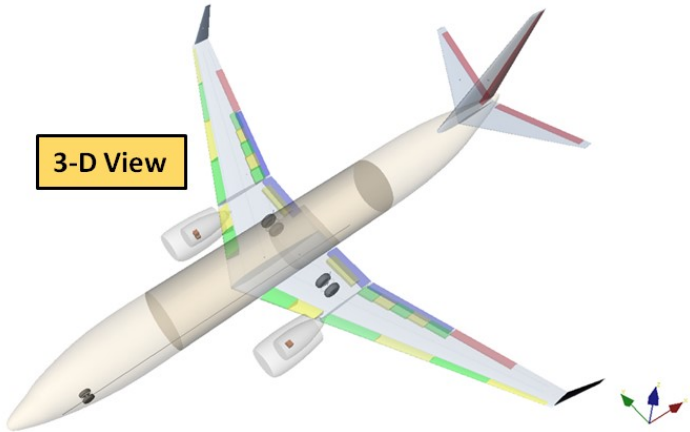

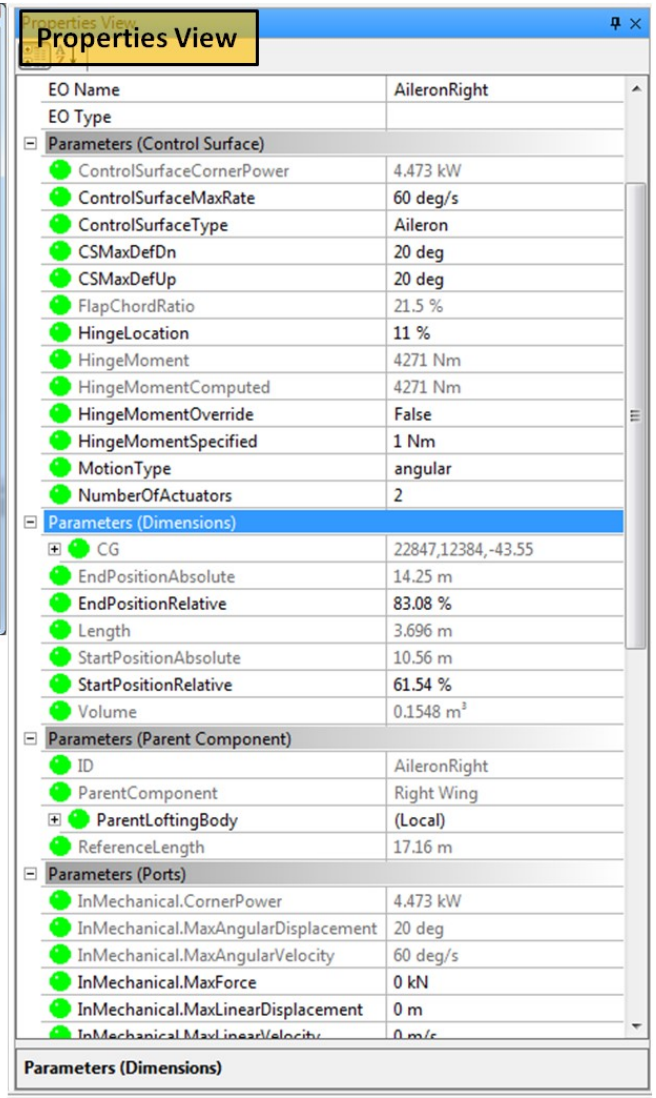

Predicted vs. published actuator weights (Aviation 2013)

Table 5. EHA Weight Estimate - Calibration

Program	F-18 SRA flaperon	Typical tandem EHA
Source	Navarro[4]	Sadeghi & Lyons[47]
Stall load (lbf)	13,300	32,000
No load rate (in/s)	7.7	8.0
Stroke (in)	4.5	-
Architecture	1 3ϕ PMM $\rightarrow$ 1 FDP	Dual EH channel, 2 TC/surface
Published weight (lb)	41.5	159.5
Predicted weight (lb)	42	164

Table 6. EMA Weight Estimate - Calibration

Program	F-18 SRA flaperon	Transport spoiler	C-141 aileron
Source	Jensen et al.[5]	Fronista & Bradbury[42]	Thompson[3]
Stall load (lbf)	13,200	50,000	19,050
No load rate (in/s)	6.7	7.0	4.65
Stroke (in)	4.125	6.0	5.43
Architecture	2 3ϕ BLDCM $\rightarrow$ 1 BS	1 5ϕ SRM $\rightarrow$ 1 BS	2 M/GB $\rightarrow$ 1 BS
Published weight (lb)	26	39	35
Predicted weight (lb)	26	40	37

Chakraborty, I., Jackson, D., Trawick, D., and Mavris, D.N., ***"Development of a Sizing and Analysis Tool for Electrohydrostatic and Electromechanical Actuators for the More Electric Aircraft"***, AIAA Aviation 2013 Conference, Los Angeles, California, August 12-14, 2013, AIAA-2013-4282

Chakraborty, I., Trawick, D., Jackson, D., and Mavris, D.N., ***"Electric Control Surface Actuator Design Optimization and Allocation for the More Electric Aircraft"***, AIAA Aviation 2013 Conference, Los Angeles, California, August 12-14, 2013, AIAA-2013-4283

Back

Weight Comparison between Config 1 & 2 (SciTech 2014)

Table 7. Weight comparison between Configuration 1 and Configuration 2

Control surface Actuators			Config. 1 Weight (kg)			Config. 2 Weight (kg)		
Name	#	Act./surf.	Design	Unit	Group	Design	Unit	Group
Aileron	2	2	EHA	15.8	63.2	EHA	15.8	63.2
Elevator	2	2	EHA	25.6	102.4	EHA	25.6	102.4
Rudder	1	3	EHA	27.0	81.0	EHA	27.0	81.0
Flight spoiler	8	1	EHA	10.2	81.6	EMA	9.0	72.0
Ground spoiler	4	1	EHA	8.4	33.6	EMA	8.9	35.6
Krueger flap	4	1	EHA	19.9	79.6	EMA	13.4	53.6
LE slat	8	1	EHA	16.3	130.4	EMA	9.7	77.6
TE flap	4	2	EMA-LS	44.5	356.0	EMA-LS	44.5	356.0
Total Weight of Actuators →			Total →		**927.8**	Total →		**841.4**
Electrical Wiring			Len.(m)	AWG	Wt.(kg)	Len.(m)	AWG	Wt.(kg)
			571	4/0	544	571	4/0	544
Total Architecture Weight →			Total →		**1471.8**	Total →		**1385.4**

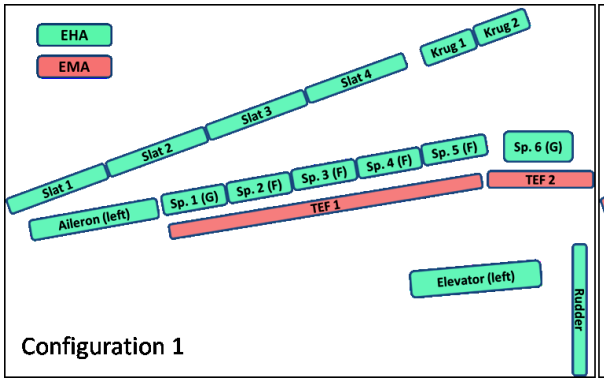

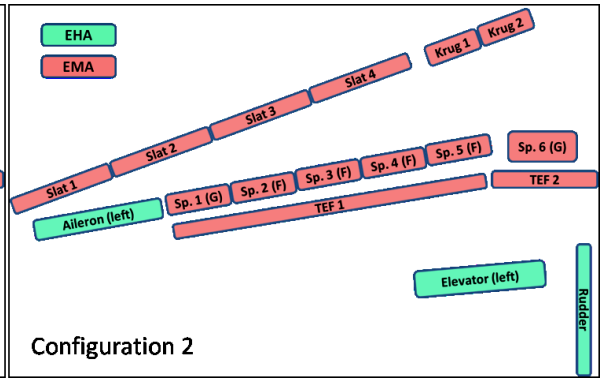

Chakraborty, I., Mavris, D.N., Emeneth, M., and Schneegans, A., ***"A System and Mission Level Analysis of Electrically Actuated Flight Control Surfaces using Pacelab SysArc"***, AIAA Science and Technology Forum and Exposition (SciTech) 2014, National Harbor, Maryland, Jan 13-17, 2014, AIAA-2014-0381

Back

Wheel Braking

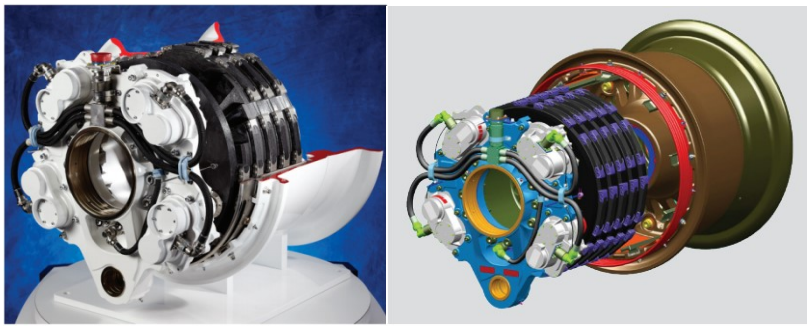

"Goodrich 787 Electro-Mechanical Brake", available online: http://utcaerospacesystems.com/cap/Documents/

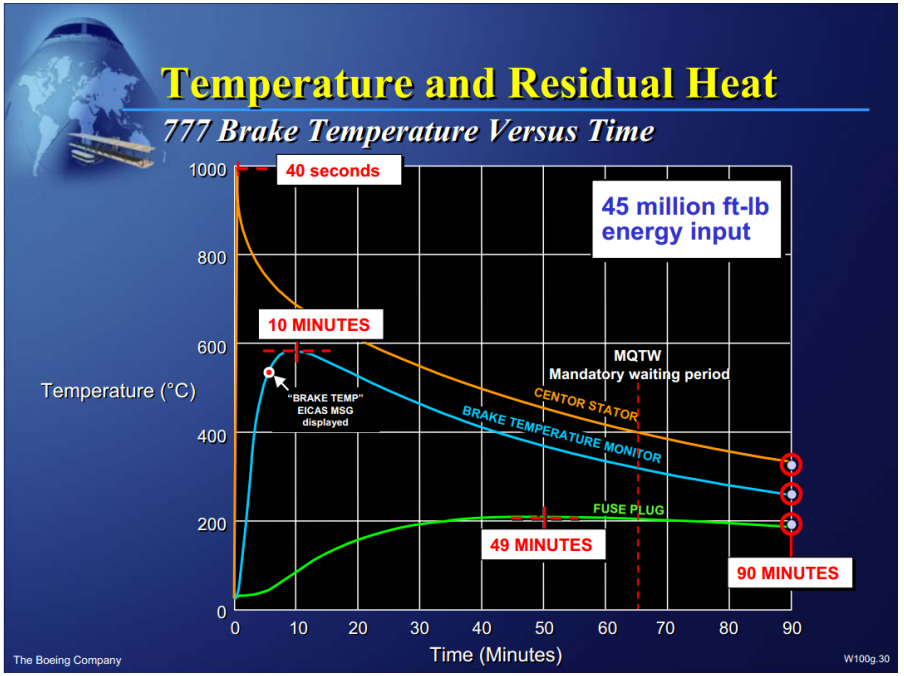

Rob Root, ***"Brake Energy Considerations in Flight Operations"***, Flight Operations Engineering, Boeing Commercial Airplanes, September 2003, available online: www.smartcockpit.com

Back

Nose-wheel steering moment (ELGEAR project)

- **Supply voltage:** ± 270V dc.
- **Peak torque:** 7000Nm
- **Max operating speed:** 18.5°/sec
- **Peak output power:** ~1kW

*** A320 variant was not specified.**

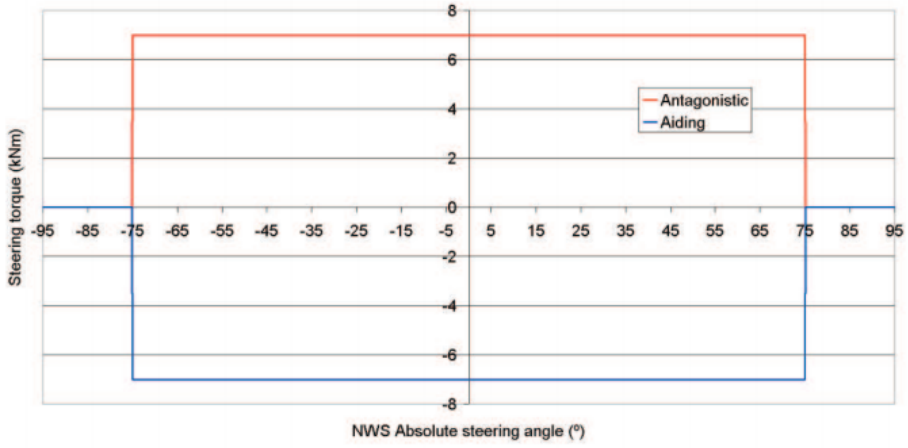

Figure 2-10: Torque/angle profile for ELGEAR NWS.

Ramp weight vs. predicted steering moment

MRW (kg)	Moment (Nm)
68,400 (A320-100)	7,270
79,229 (B737-800)	8,421

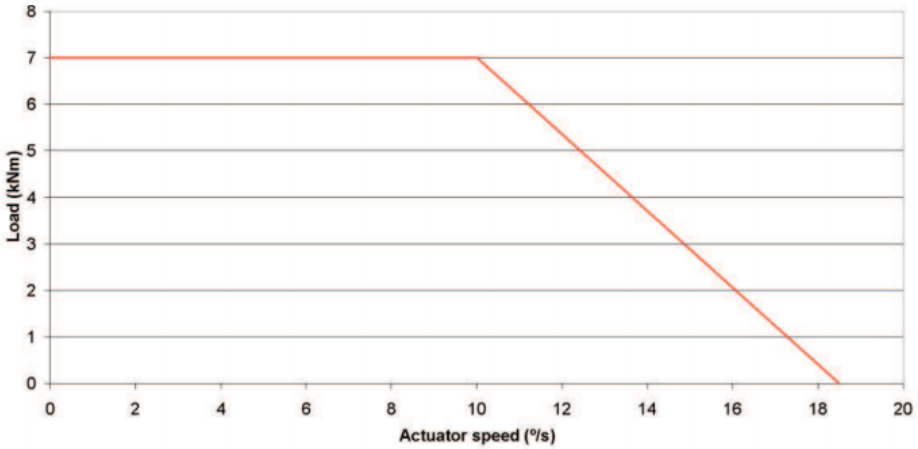

Figure 2-11: Torque/speed profile of ELGEAR actuator.

Back

Air Cycle Machine Characteristics

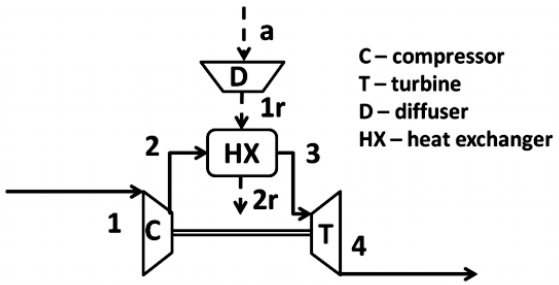

Table 14. Air Cycle Machine parameters

Parameter	Symbol	Value
Compressor efficiency	η_c	0.75
Turbine efficiency	η_t	0.80
Ram diffuser efficiency	η_{rd}	0.95
Pack air $\Delta P/P$	μ_h	0.18
Ram air $\Delta P/P$	μ_c	0.06
HX max effectiveness	ϵ_{max}	0.80

Pack air stream:

$$T_2 = T_1 \left(1 + \frac{1}{\eta_c}\left(CPR^{\frac{\gamma-1}{\gamma}} - 1\right)\right) \quad (26)$$

$$\left(\frac{1}{TPR}\right)^{\frac{\gamma-1}{\gamma}} = 1 - \frac{1}{\eta_t}\left(1 - \frac{T_4}{T_3}\right) \quad (27)$$

$$\dot{W}_t = \dot{W}_c \implies T_3 - T_4 = T_2 - T_1 \quad (28)$$

$$\frac{P_1}{P_4} = \frac{P_1}{P_2} \cdot \frac{P_2}{P_3} \cdot \frac{P_3}{P_4} = \frac{TPR}{CPR} \cdot \frac{1}{1-\mu_h} \quad (29)$$

Ram air stream:

$$T_{1r} = T_a \left(1 + \frac{\gamma - 1}{2} M^2\right) \quad (30)$$

$$P_{1r} = P_a \left(\eta_{rd}\left(\frac{T_{1r}}{T_a} - 1\right)\right)^{\frac{\gamma}{\gamma-1}} \quad (31)$$

$$P_{2r} = P_{1r}\left(1 - \mu_c\right) \quad (32)$$

$$\epsilon = \frac{T_2 - T_3}{T_2 - T_{1r}} \quad (33)$$

$$\epsilon = 1 - \exp\left(\lambda (NTU)^{0.22}\left(\exp\left(-\lambda^{-1} NTU^{0.78}\right) - 1\right)\right) \ldots (\text{solve } \lambda) \quad (34)$$

$$\dot{m}_{ram} = \lambda\, \dot{m}_{pack} \quad (35)$$

$$T_{2r} = T_{1r} + \frac{T_2 - T_3}{\lambda} \quad (36)$$

Cabin Air Distribution & Recirculation Schematics

Electric ECS Architecture

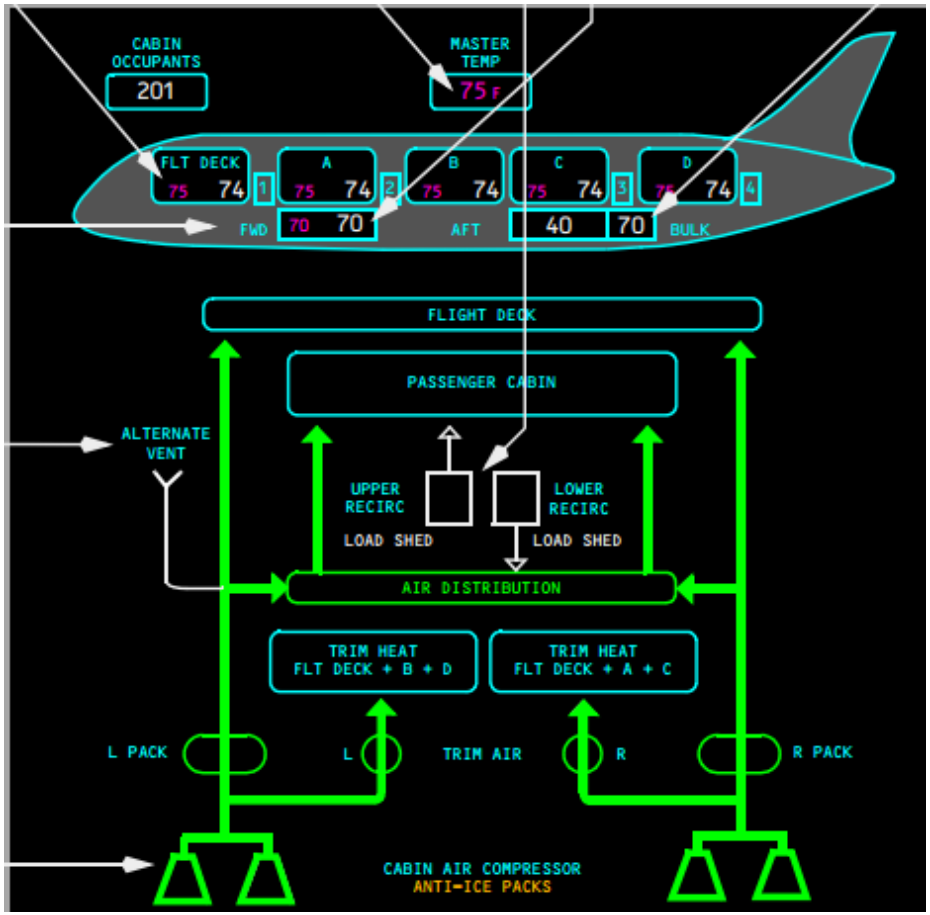

Boeing 787-8 Flight Crew Operations Manual – The Boeing Company

Conventional ECS Architecture

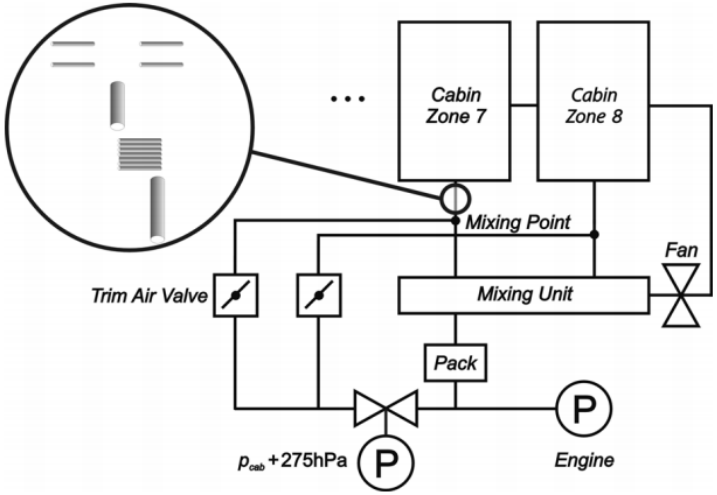

Muller C., Scholz, D., Giese, T., ***"Dynamic Simulation of Innovative Aircraft Air Conditioning"***, First CEAS European Air and Space Conference, Berlin, Sept. 10-13, 2007, Paper: CEAS-2007-466, ISSN 0700-4083

Back

Fuel Savings vs. Risk, A320 (Jones, 2002)

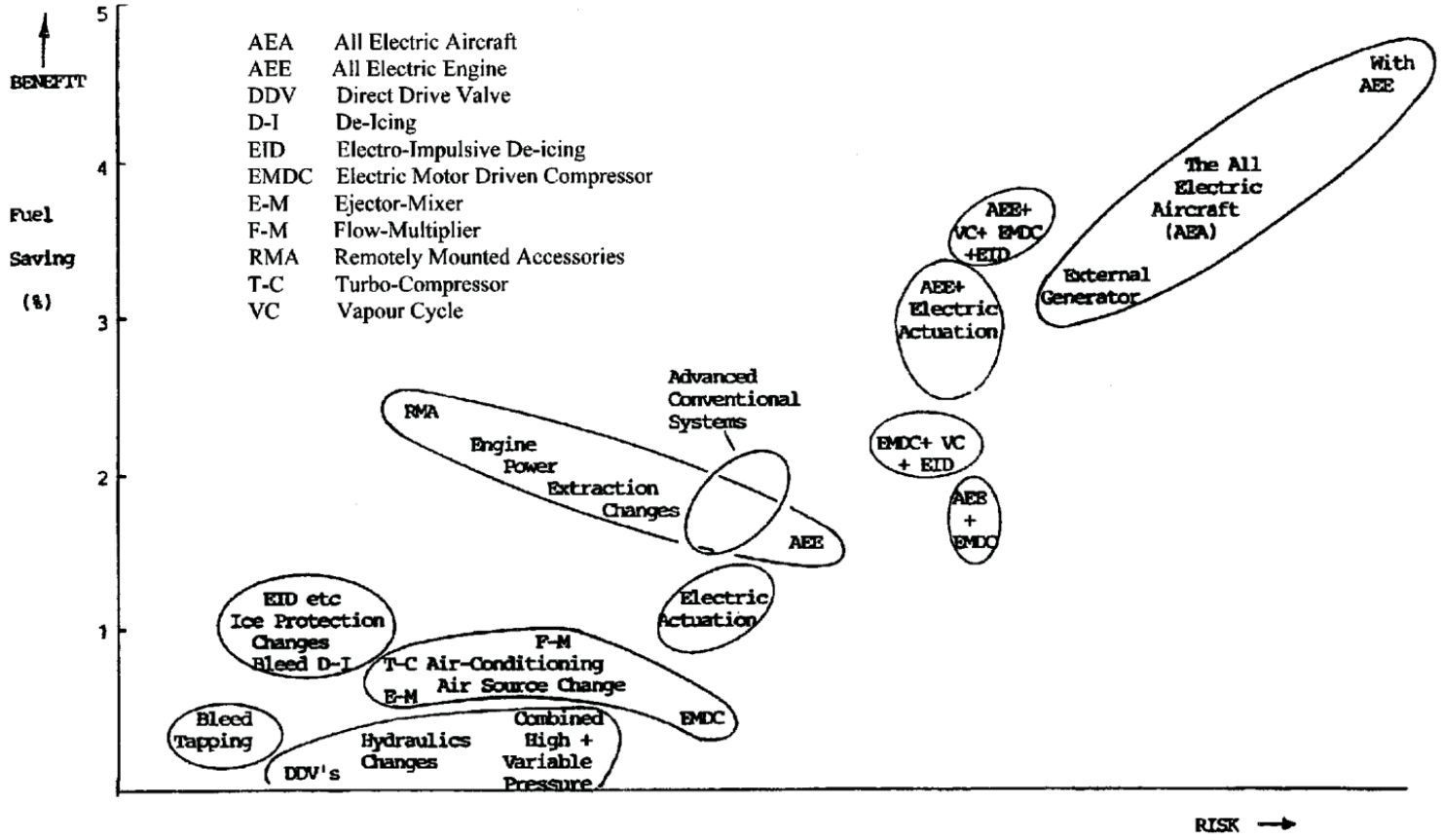

Fig. 6 Fuel savings relative to risks involved in adoption of changes considered on an A320

Jones, R., ***"The More Electric Aircraft - Assessing the Benefits,"*** Proceedings of the Institution of Mechanical Engineers, Part G, Journal of Aerospace Engineering, Vol. 216, 2002, pp. 259–270

Back